Supplemental Material

Plasmacytoid dendritic cells in lung and skin fibrosis in bleomycin-induced model and patients with systemic sclerosis

S. Kafaja, I. Valera, A.A. Divekar, R. Saggar, F. Abtin, D.E. Furst, D. Khanna, R.R. Singh

Correspondence to: RRSingh@mednet.ucla.edu

Supplemental Tables

Supplemental Figures

Supplemental Materials and Methods

Supplemental References

Table S1. **Demographic and clinical characteristics of human subjects in the study**

A. Peripheral blood studies

Peripheral blood was obtained from 30 subjects, including 15 randomly selected patients with SSc and the same number of healthy donors who were matched with the patients for sex/race/ethnicity and age (± 5 years).

	SSc	**Healthy Donors**
Age (years), Mean (SD)	45.6 (12.5)	44.5 (10.7)
Disease duration (years), Mean (SD)	6.4 (3.2)	–
Gender: N (%)		
Female	11 (73.3)	11 (73.3)
Race/ethnicity: N (%)		
White	7 (47)	7 (47)
Asian	5 (33)	5 (33)
Hispanic	3 (20)	3 (20)
Diffuse SSc: N (%)	14 (93)	–
ILD: N (%)	12 (80)	–
mRSS (0-51), Mean (SD)	21.2 (8.1)	–

B. BAL studies

BAL samples were collected from the right middle and lower lobes (RML and RLL) of 21 subjects, including 15 SSc patients who were participants in a single center, open-label study of imatinib for the treatment of SSc-ILD (1) and had a bronchoscopy at the baseline. 11 of these patients had their BAL collected at the end of one-year trial. BAL samples from 6 patients with a primary diagnosis of vasculitis, connective tissue disease, or lung nodules who had bronchoscopy for respiratory symptoms but were found to have no significant lung disease on further diagnostic work-up, including imaging and/or biopsy, and clinical evaluations by their pulmonologists were used as controls.

	SSc	**Controls**
Age (years), Mean (SD)	44.0 (12.4)	46.4 (19.8)
Disease duration (years), Mean (SD)	4.2 (2.9)	2.9 (8.5)
Gender: N (%)		
Female	11 (73.3)	4 (66.7)
Race/ethnicity: N (%)		
White	10 (66.7)	4 (66.7)
Asian	3 (20.0)	
Hispanic	2 (13.3)	2 (33.3)
mRSS (0-51), Mean (SD)	19.5 (10.2)	–
FVC% predicted (%), Mean (SD)	66.2 (15.4)	–
DLCO% predicted (%), Mean (SD)	51.4 (11.2)	–
TLC% predicted (%), Mean (SD)	74.5 (11.2)	–

C. Lung tissues for immunohistochemistry studies

Lung tissue sections from 15 subjects were obtained from Translational Pathology Core, which included 8 lung explants with SSc-ILD and pulmonary arterial hypertension. Seven non-SSc, control lung tissues were the wedge resections from patients with spontaneous pneumothorax or lung laceration after a traumatic fall

or histologically normal lung tissue on autopsy from patients who died of renal cancer, primary biliary cirrhosis, and hepatitis B liver cirrhosis. Biopsy sections were stained twice.

	SSc	Controls
Age (years), Mean (SD)	50.6 (7.9)	58.8 (13.2)
Disease duration (years), Mean (SD)	9.3 (2.9)	–
Gender: N (%)		
Female	5 (62.5)	5 (71.4)
Race/ethnicity: N (%)		
White	3 (37.5)	5 (71.4)
Asian	1 (12.5)	
Hispanic	4 (50)	
Black		2 (28.6)
Diffuse SSc: N (%)	3 (37.5)	–
Histological changes of usual interstitial pneumonia (UIP) pattern of pulmonary fibrosis: N (%)	8 (100)	–
Histological changes of pulmonary hypertension: N (%)	8 (100)	–

D. Skin biopsies for immunohistochemistry studies

Skin biopsies from 6 heathy volunteers and 7 patients with early SSc. Biopsy sections were stained twice. Healthy volunteers were 36–74-year-old, all White.

	SSc
Age (years), Mean (SD)	45.4 (15.6)
Disease duration, years	< 5 years since first non-Raynaud symptoms
Gender: N (%)	
Female	5 (71.4)
Race/ethnicity: N (%)	
White	4 (57.1)
Asian	1 (14.3)
Hispanic	2 (28.6)
Diffuse SSc: N (%)	7 (100)
ILD: N (%)	4 (57.1)
mRSS (0-51), Mean (SD)	30.7 (7.65)

DLCO, diffusing capacity of lung for carbon mono-oxide; FVC, forced vital capacity; ILD, interstitial lung disease; mRSS, modified Rodnan Skin Score; SSc, systemic sclerosis; TLC, total lung capacity.

Table S2. **Quantitation of fibrosis and GGO on HRCT scans in SSc patients presented as percentage of the lobe involved**

Patient number	Fibrosis		GGO	
	RML (%)	RLL (%)	RML (%)	RLL (%)
1	10	7	30	35
2	1	4	10	60
3	5	20	10	35
5	10	30	30	70
6	5	15	5	5
7	1	7	1	7
8	3	5	0	3
9	10	30	10	20
10	50	50	20	20
11	0	5	0	7
12	0	0	0	10
13	0	2	0	2
14	0	2	0	5
15	40	65	5	6

HRCT scans of lung were performed in 14 of 15 patients enrolled in an open label study for imatinib mesylate. Pt#4 did not have a baseline HRCT. The HRCT scans at baseline were quantitated for GGO and fibrosis, as described in Supplemental Fig. S7. Note that the HRCT scores were substantially different between RML and RLL in most patients.

GGO, ground glass opacity; HRCT, high resolution computerized tomography; RLL, right lower lobe; RML, right middle lobe.

Fig. S1. An injection of anti-PDCA1 Ab reduces pDCs, but not mDCs, and T and B cells, in naïve mice.

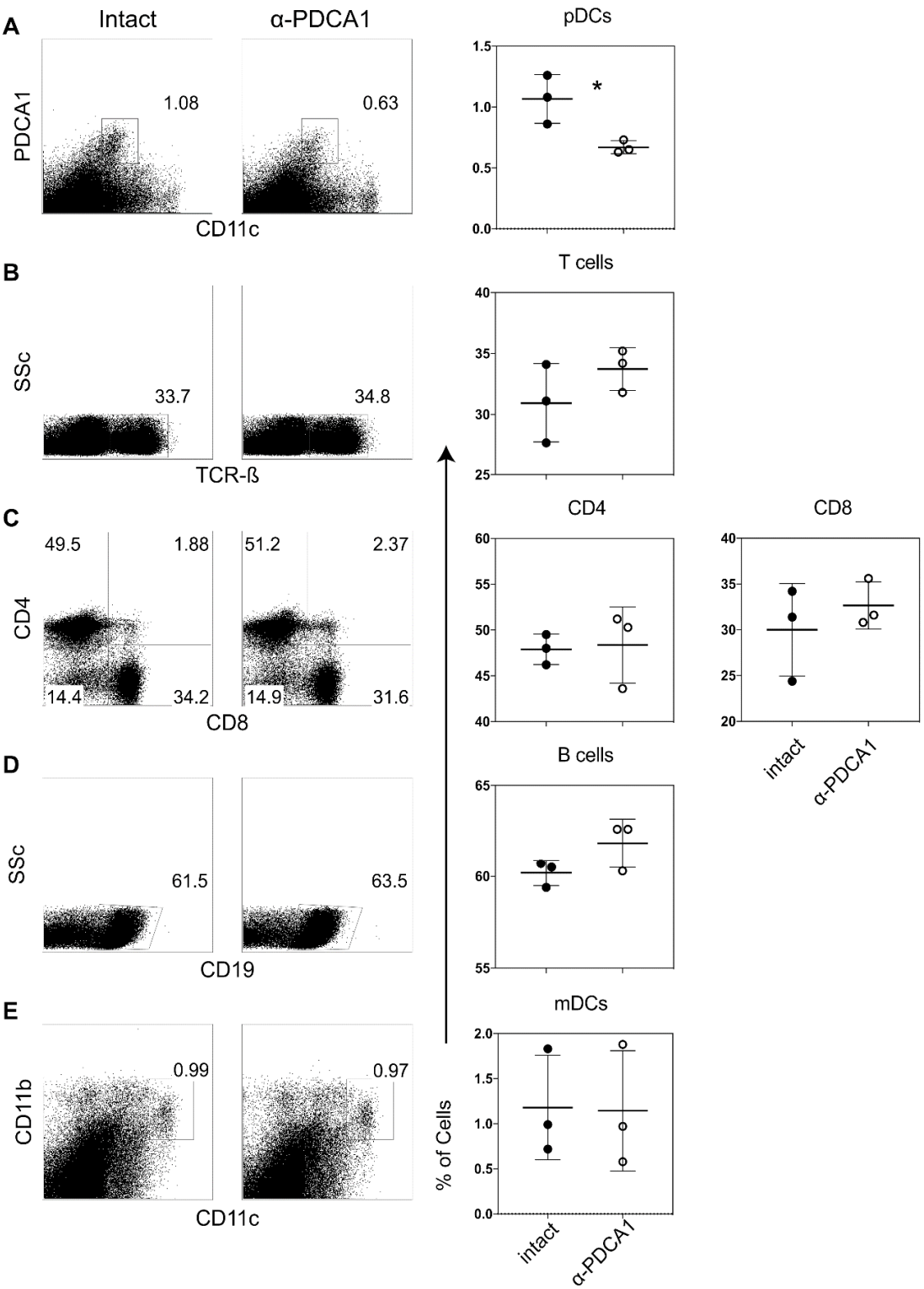

Naïve C57/BL6 mice were injected i.p. with 100 µg of anti-PDCA1 Ab or an isotype-matched control IgG. Spleen was harvested on d 3, and single cell suspensions stained for immune cell types as indicated on the panels. Results are shown as representative FACS plots, and symbol plots with each symbol representing value from an animal and as the mean ± SEM. *$p<0.05$, unpaired t-test.

Fig. S2. Depletion of pDCs using an anti-PDCA-1 Ab in bleomycin-injected mice.

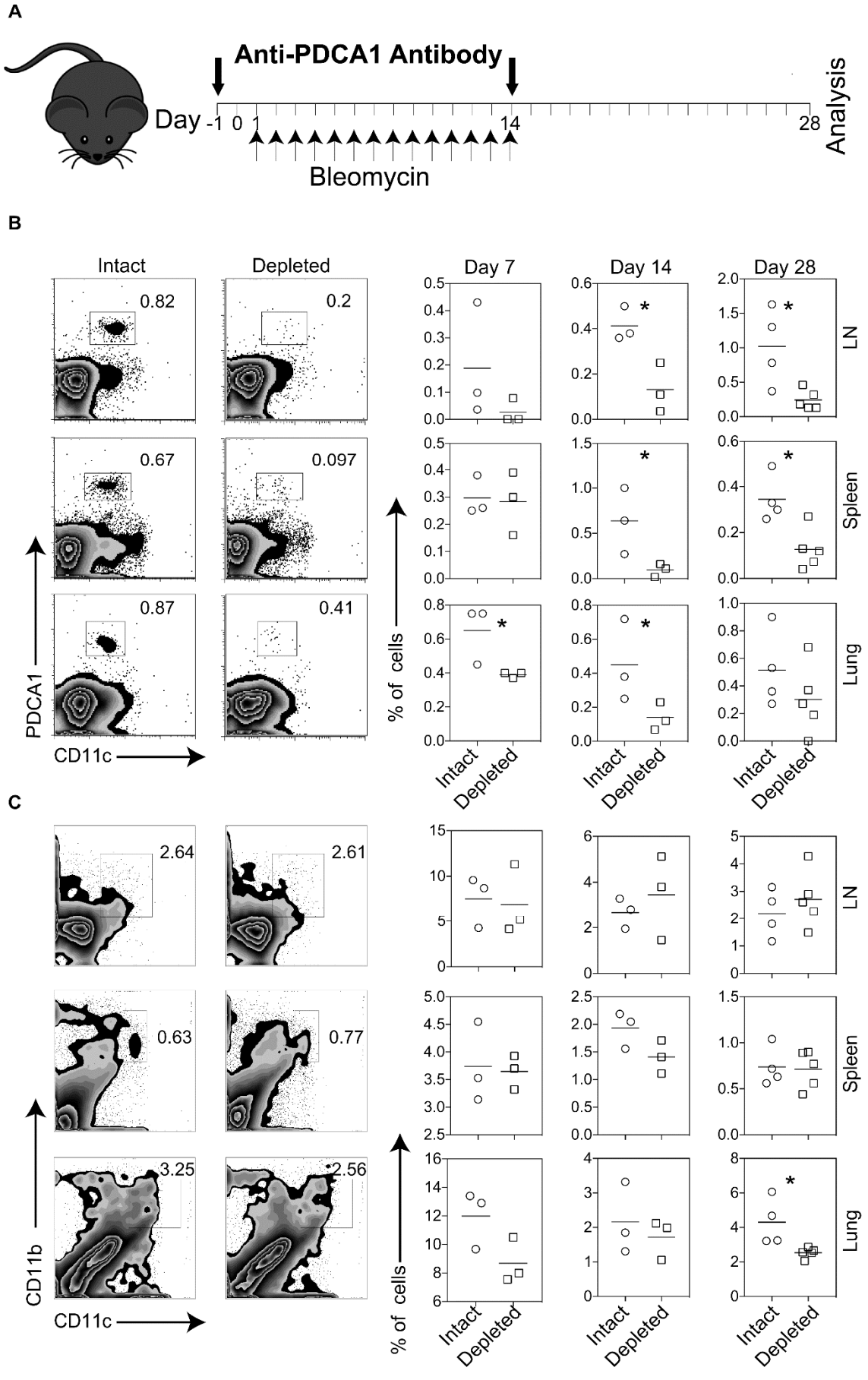

Animals (n = 21) were injected s.c. with bleomycin for two consecutive weeks (d 1 to d 14). On d –1 and d 14, the animals received i.p. injections, 100 μg each, of anti-PDCA1 Ab or of isotype-matched control IgG (**A**). Lung-draining lymph nodes (LN), spleen and lungs were harvested at the indicated timepoints, and their single cell suspension stained to detect pDCs, as live $SSc^{low}FSC^{low}$ $CD19^{-}B220^{+}$ $CD11c^{int}PDCA1^{+}$cells (**B**) and mDCs, as live $CD11b^{+}CD11c^{+}$ cells (**C**). Results are shown as representative FACS plots and symbol plots. Each symbol represents an animal. Small horizontal lines denote average values. Results are representative of five independent experiments, each using 4-5 animals per group. *$p<0.05$. Mann-Whitney U-test.

The frequency of pDCs in all organs tested were lower in anti-PDCA1 Ab treated mice (*Depleted*) than in isotype IgG injected control mice (*Intact*), whereas mDCs were only reduced in the lungs of pDC-depleted mice at d 28, when these mice have reduced lung disease (Figure 2) and reduced immune cell infiltration (Figure 4).

Fig. S3. Effect of anti-PDCA1 Ab treatment after the induction of bleomycin-induced disease.

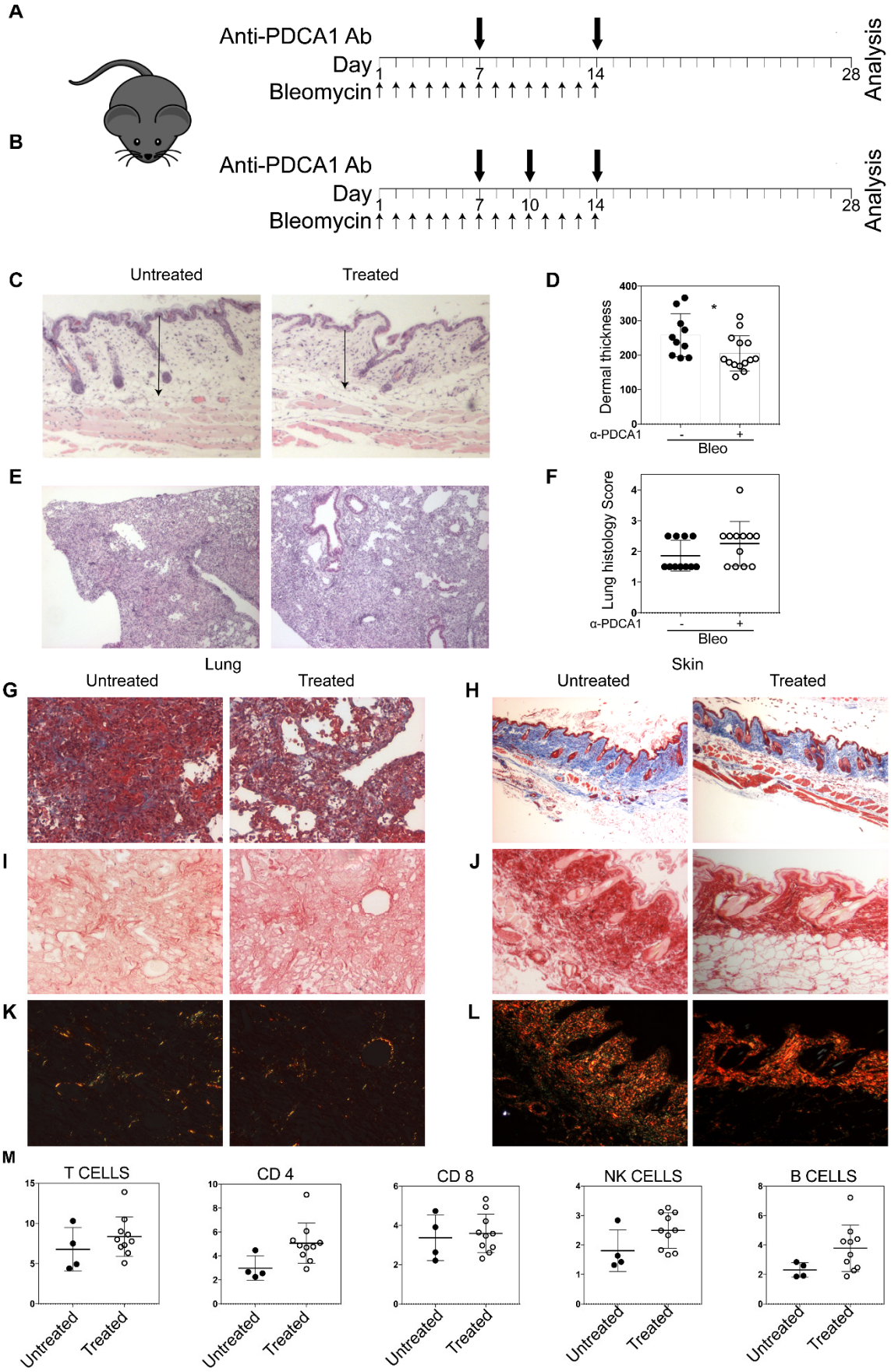

(**A**, **B**) Animals were injected s.c. with bleomycin for two consecutive weeks (d 1 to d 14). On d 7 and 14, animals received i.p. injections, 200 μg each, of anti-PDCA1 Ab (*Treated*) or were left untreated (*Untreated*). Another set of animals received three injections, 100 μg each, of anti-PDCA1 Ab on d 7, 10, and 14. A total of 24 animals were treated with anti-PDCA1 Ab, including 18 mice with two injections and 6 with three injections, in two separate experiments. 12 untreated animals served as controls. Animals were monitored for 28 d, and skin and lungs harvested for histology and flow cytometry studies. Stained tissue sections were blindly read by three investigators (IV, SK, and RRS). (**C**, **D**) Dermal thickness was measured as indicated by arrows in the representative photomicrographs of H&E stained sections of skin from the untreated and treated animals. Dermal thickness values in μm are shown as symbol plots from individual animals and as the mean ± SEM. Magnification 4X. *$p<0.05$ (unpaired t-test). (**E**, **F**) Lung sections stained with H&E were scored for the severity of lung disease. Results are shown as representative photomicrographs and as average histology scores from individual animals and as the mean ± SEM. Magnification 10X. (**G**, **H**) Lung and skin sections were stained with Masson's trichrome. Representative photomicrographs are shown (n = 10 untreated and 14 treated animals). Magnification 10X lung, 4X skin. Results show reduced trichrome staining (fibrosis) in the skin of treated animals as compared to untreated animals, but there were no differences in trichrome staining of lungs between treated and untreated animals. (**I-L**) Picro-sirius red stain imaged in parallel light to display total collagen content (**I**, **J**) or orthogonal light to display fibrillary collagen (**K**, **L**). Representative photomicrographs are shown (n = 14 treated and 10 untreated animals). Magnification 10X lung, 4X skin. Results show reduced total collagen and fibrillary collagen in the skin of treated animals as compared to untreated animals, but there were no differences in collagen content of lungs between treated and untreated animals. (**M**) Cells isolated from the lungs were stained with conjugated Ab for TCRβ, CD4, CD8, NK1.1, and CD19. Results are expressed as % positive of all live cells.

Fig. S4. Effect of anti-PDCA1 Ab treatment on pDCs after the induction of bleomycin-induced disease.

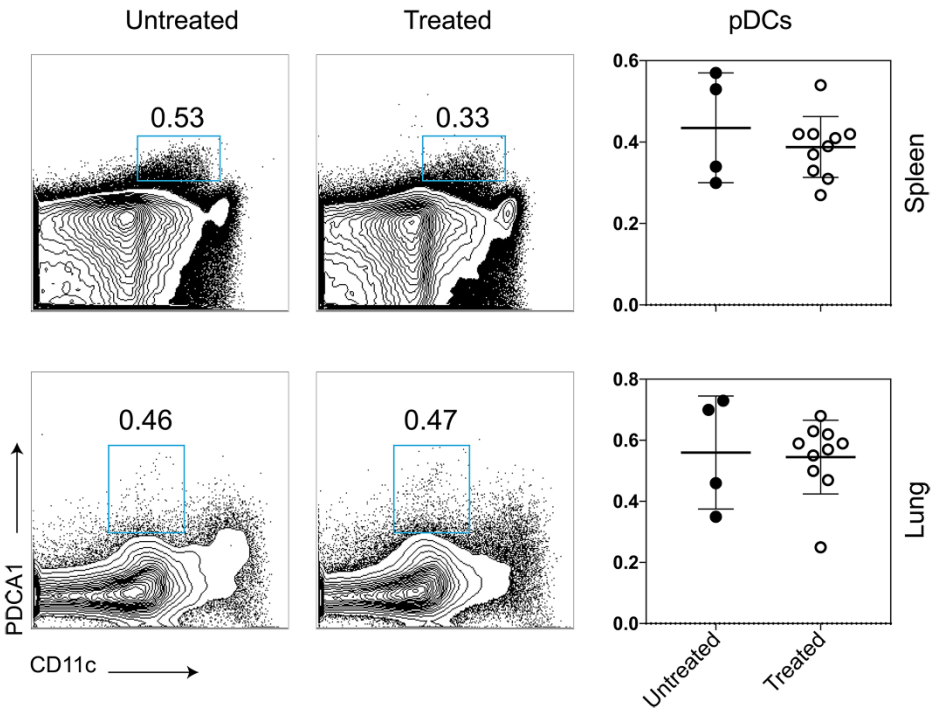

Animals were injected s.c. with bleomycin for two consecutive weeks (d 1 to d 14). On days 7 and 14, animals received i.p. injections, 200 µg each, of anti-PDCA1 Ab (*Treated*) or were left untreated (*Untreated*). Spleen and lungs harvested on d 28 from these animals were analyzed for pDCs by flow cytometry, as in Figure 1. Results are shown as representative FACS plots, and symbol plots with each symbol representing value from an animal and as the mean ± SEM (p = NS).

Results show that when the treatment was initiated 7 days after induction of bleomycin-induced disease, the frequency of pDCs on d 28 was not significantly lower in animals treated with anti-PDCA1 Ab than in untreated controls. In contrast, treatment with the same Ab depleted pDCs when it was started a day prior to administering bleomycin (100 µg on d -1 and d14; Fig S2) or when given to naïve mice (100 µg x 1; Fig. S1). Studies are underway to determine optimal regimen(s) to deplete pDCs that accumulate in the lungs of diseased mice.

Fig. S5. Gene function network analysis of differentially expressed genes in the lung and skin of pDC-depleted versus intact mice.

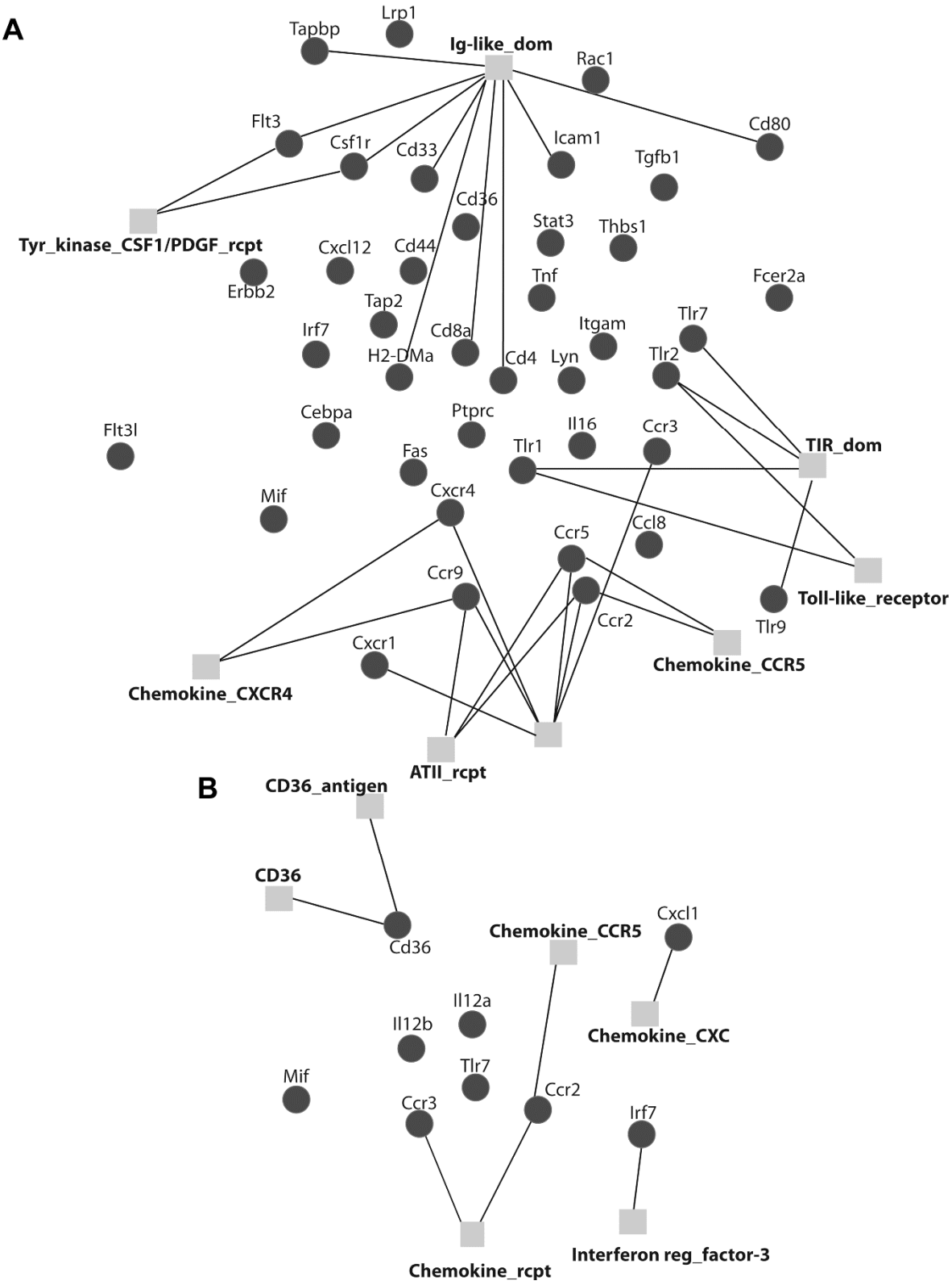

Gene function network analysis of differentially expressed genes in the lung (**A**) and skin (**B**) were analyzed using GeneMANIA (2). GeneMANIA is a flexible, web interface for generating hypotheses about gene function, analyzing gene lists, and prioritizing genes for functional assays. Given a query list, GeneMANIA

extends the list with functionally similar genes that it identifies using available genomics and proteomics data. GeneMANIA also reports weights that indicate the predictive value of each selected data set for the query.

Results show the interaction of genes classified into families with shared protein domains for biological processes (InterPro Protein Sequence Analysis and Classification: https://www.ebi.ac.uk/interpro/). The top 10 families for differentially expressed genes between pDC-depleted and intact animals included Ig-like domains, which included proteins involved in cell-cell recognition, cell-surface receptors, muscle structure, and the immune system; Toll proteins or Toll-like receptors (TLRs) and the interleukin-1 receptor (IL-1R) superfamily, both involved in innate immunity; ATII receptor that is responsible for the signal transduction of the vasoconstricting stimulus of the main effector hormone, angiotensin II; CC chemokine receptor 5 (CCR5) found on the surface of macrophages, T cells, and dendritic cells, and expressed in lymphoid organs; chemokine receptors that are preferentially expressed on dendritic cell subsets, monocytes and lymphocytes, and T helper cells, and can be subclassified into homeostatic leukocyte homing molecules (CXCR4 and CCR9) versus inflammatory/inducible molecules (CXCR1); and CD36 that recognizes oxidized low density lipoprotein, long chain fatty acids, anionic phospholipids, collagen types I, IV and V, and thrombospondin (TSP), and is involved in platelet adhesion and aggregation, platelet-monocyte interaction, and in directing monocytes along the endothelium during vascular damage.

Fig. S6. Myeloid DC (mDC) in the peripheral blood of patients with SSc and healthy donors.

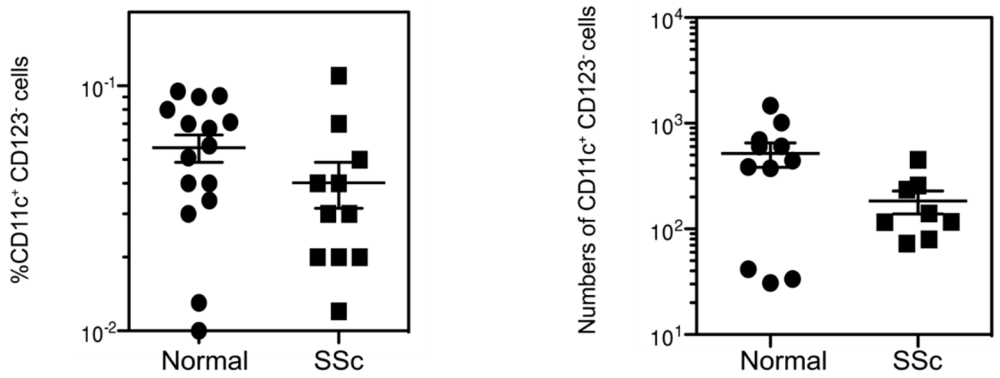

Peripheral blood mononuclear cells from 15 each of healthy controls and SSc patients were stained for cell surface markers of DC: CD11c, CD123, HLA-DR and BDCA-2. mDCs were defined as live $CD11c^+$ $HLA\text{-}DR^+$ $CD123^-$ cells. Results are expressed as the percentage (left panel) and absolute numbers (right panel) of these cells. Each symbol represents an individual patient (p=NS).

Fig. S7. Radiographic definition of HRCT findings of SSc-ILD in patients.

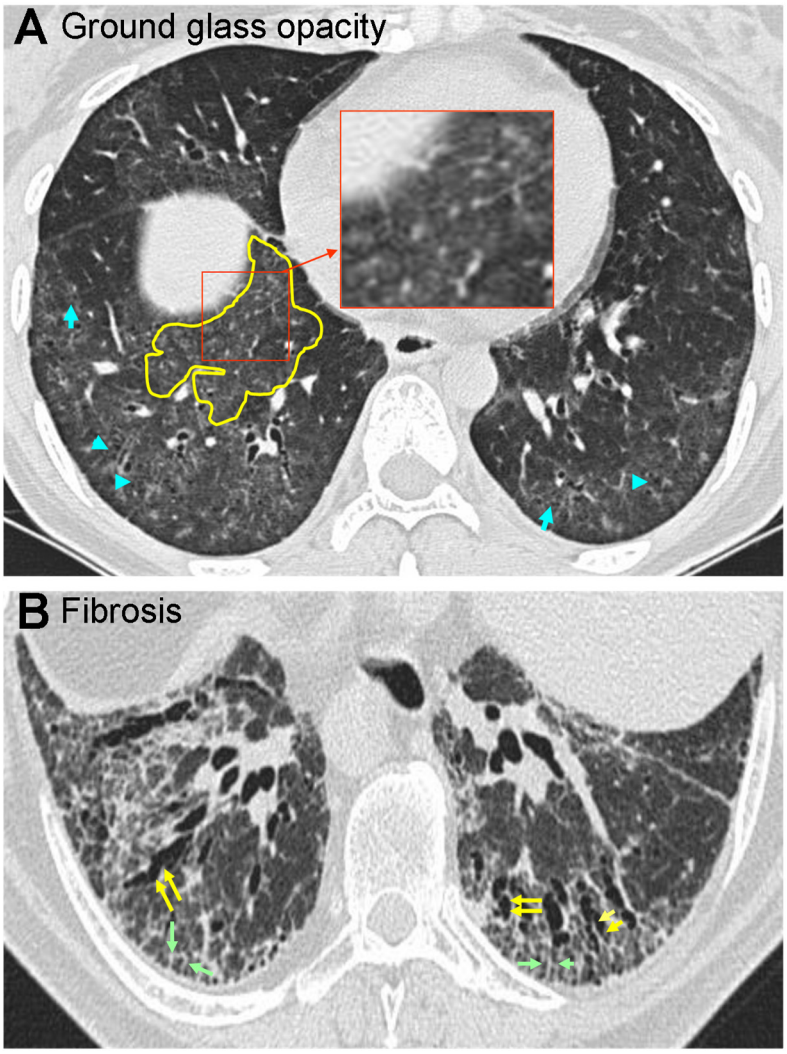

Volumetric CT scans were obtained in full inspiration and analyzed by an expert thoracic radiologist (F.A.) blinded to clinical and hemodynamic information. A linear scoring system was used. The following radiographic definitions were employed: ground-glass opacity (GGO) represents hazy parenchymal opacity in the absence of reticular opacity, or architectural distortion; lung fibrosis represents reticular opacification, traction bronchiectasis, and bronchiolectasis; and honeycombing represents clustered air-filled cysts with dense walls. Each lung was scored separately and then each of five lobes were scored separately (upper, middle and lower lobes) for each category of parenchymal abnormality: fibrosis (CT-determined fibrosis score), GGO (CT determined GGO), honeycombing (CT-determined honeycomb score]). The honeycombing was classified as predominantly microcystic (less than 4 mm cysts) and macrocystic (more than 4 mm cysts).

A. CT scan images obtained at 1 mm in supine position, demonstrating predominant GGO in both lower lobes, and parts of visualized right middle lobe. A part of GGO in right lower lobe is outlined by yellow line. Areas of coarse or textured GGO with associated bronchiectasis and bronchiolectasis (blue arrows) are considered as early fibrosis.

B. CT scan images obtained in prone position shows fibrosis as demonstrated by thickened inter and intralobular septae (green arrows), traction bronchiectasis and bronchiolectasis (yellow arrows), without honeycombing or significant GGO.

Fig. S8. Co-localization of pDCs and TGF-β in skin and lung tissues from patients with SSc.

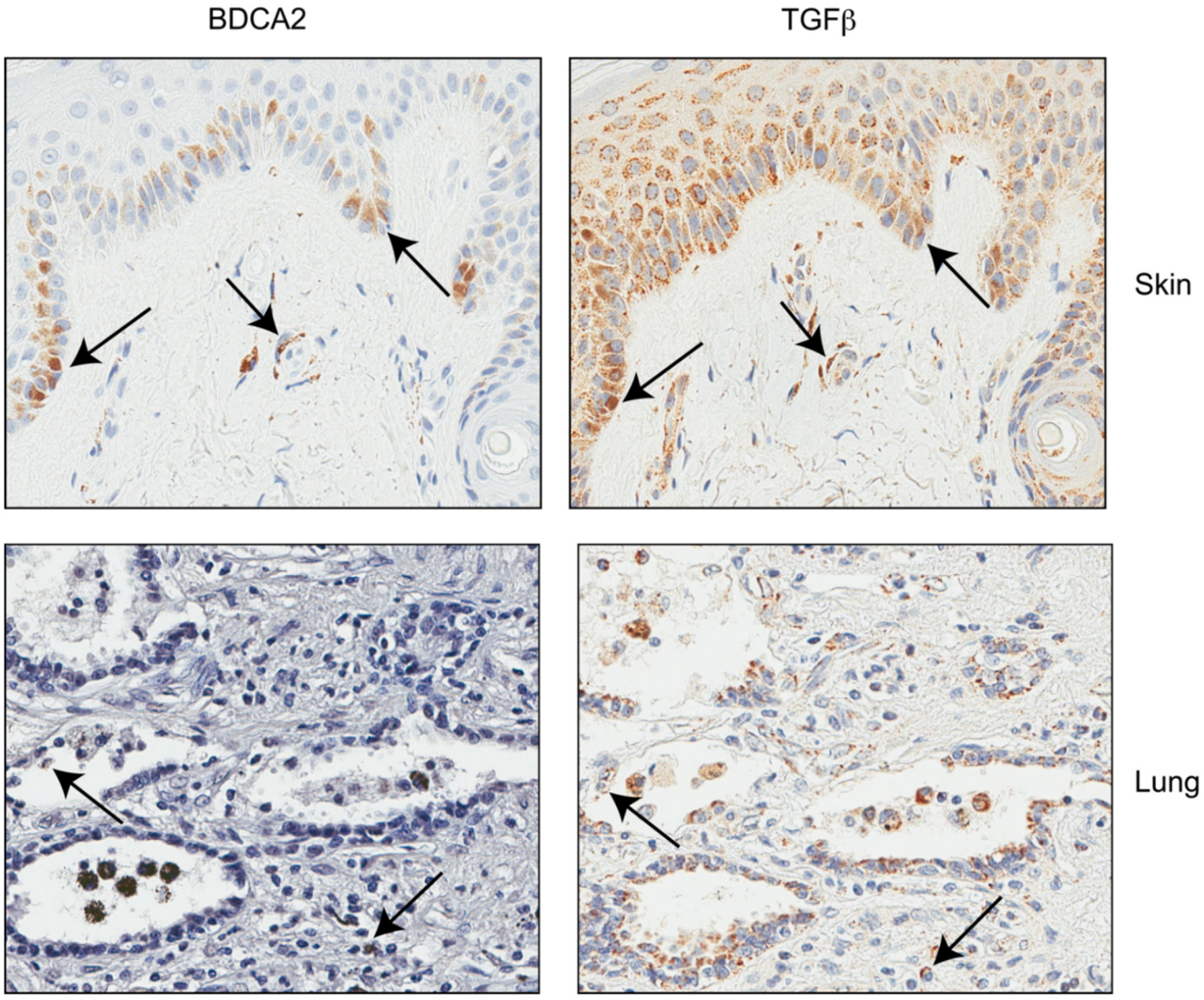

Consecutive sections of the lung and skin tissues shown in **Fig. 8** were stained for BDCA-2 and TGFβ. Representative photomicrographs are shown. Upper panels show frozen sections (6 μm) of skin biopsies from patients with SSc. Lower panels show 4 μm sections of paraffin-embedded blocks of lung tissues from SSc patients with PAH and ILD.

Fig. S9. Correlation of BAL pDCs with the BAL fluid proteins in patients with SSc.

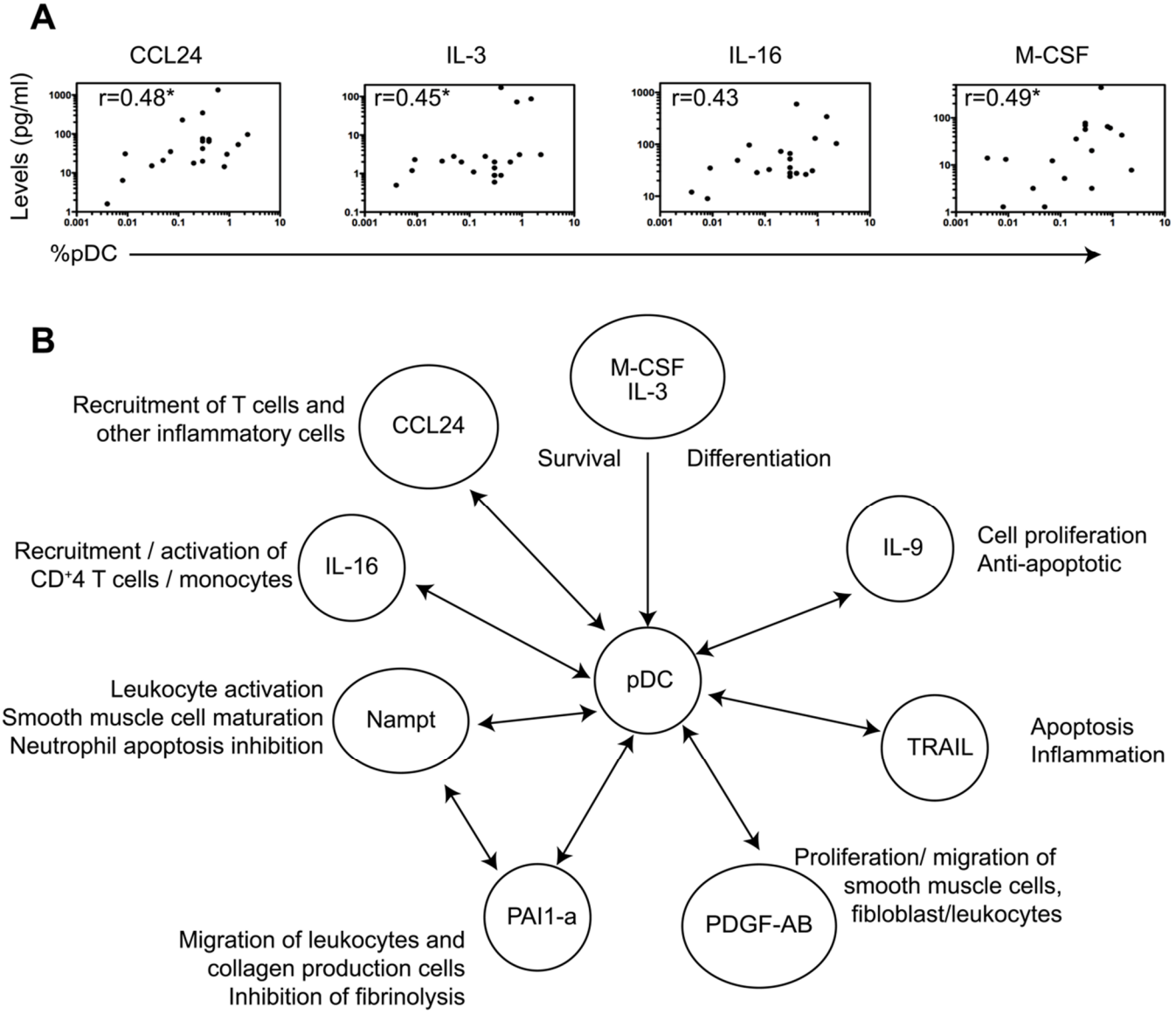

BAL was collected at the baseline in SSc-ILD patients enrolled in the imatinib trial. BAL samples were analyzed for 96 cytokines that were selected after a preliminary screening of 165 analytes for proteins that were detected in SSc BAL samples and correlated with HRCT findings in our study or reported previously to be associated with ILDs in humans and animals (R.R. Singh and colleagues, manuscript in preparation). These proteins were measured using a SearchLight multiplex protein array (Aushon Biosystems, MA). Each cytokine was run in duplicates and the mean of two readings is reported. Among the proteins that were present above the detection limit in >25% of samples, nine correlated with pDC frequency with an r ≥0.4. Four of these 9 proteins are shown as examples of proteins that correlated with the frequency of pDC in BAL (*p<0.05) (**A**).

The relevant functions of all proteins that correlated with pDCs are stated in **B**. Arrows indicate possible interactions, direct or indirect, between proteins and pDCs. Among the proteins that correlated with pDCs, IL-16 and CCL24 can serve as chemoattractants for T cells, DCs and other immune cells (3-7), M-CSF and IL-3 can potentially promote pDC differentiation and survival (8-12), PDGF and PAI1-a (plasminogen activator inhibitor-1 active form) can induce the recruitment and/or proliferation of smooth muscle cells and fibroblasts that produce extracellular matrix (13-15), and Nampt (visfatin) can cause vascular smooth muscle maturation and reduce leukocyte apoptosis (16, 17).

Fig. S10. Correlation of alterations in BAL pDC frequencies with changes in local proteins over one year (baseline–post-imatinib) in patients with SSc

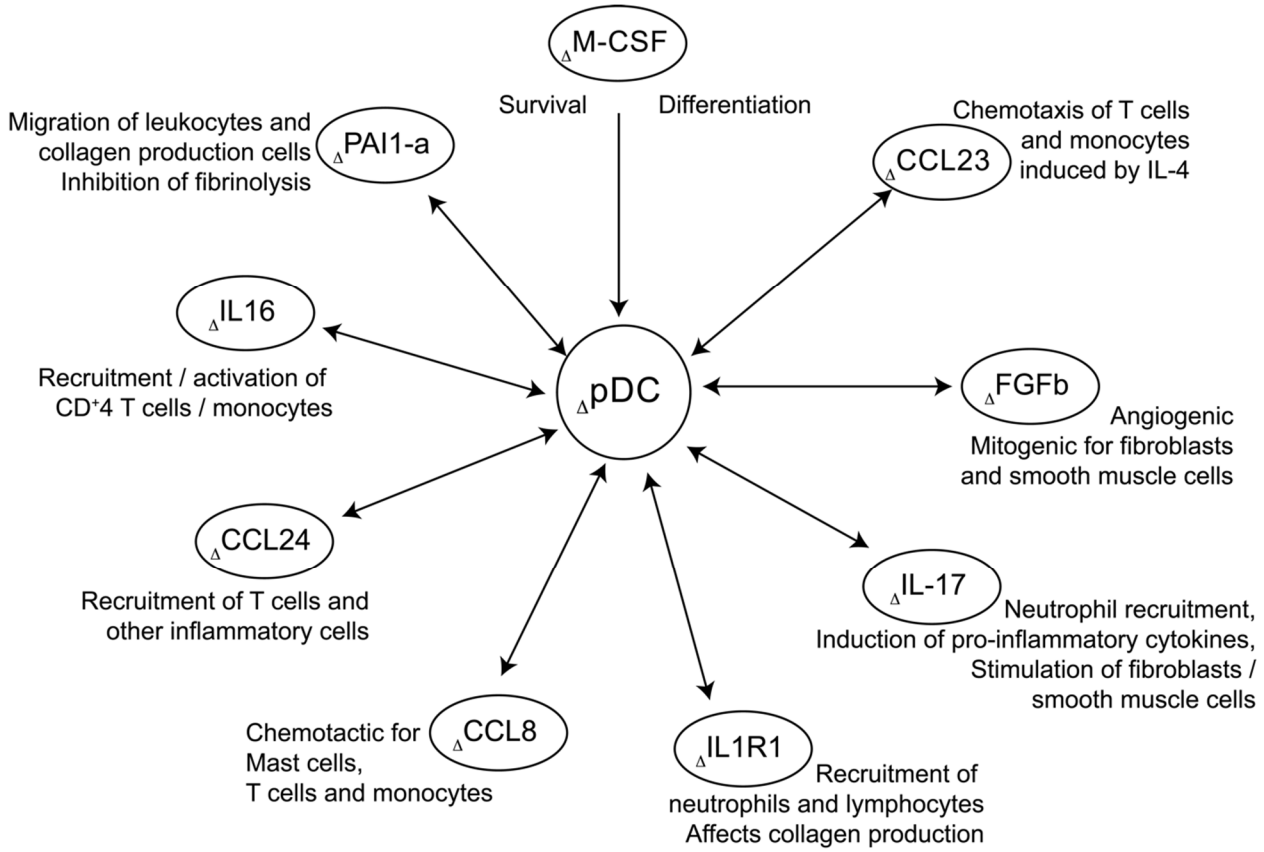

BAL samples were collected at the baseline and at one year post-treatment from SSc-ILD patients enrolled in the imatinib trial. BAL samples were available from 11 patients both at baseline and post-imatinib. These samples were analyzed for pDCs and 96 proteins, as described in **Fig. S9**. Change in pDC frequencies post-imatinib from baseline (ΔpDC) correlated with changes in local levels of nine proteins ($r \geq 0.4$), including four proteins that associated with pDCs at the baseline in **Fig. S9**.

Protein functions that are potentially relevant to ILD are briefly stated on the diagram, including cellular recruitment/chemotaxis (CCL8, CCL23, CCL24, IL-16, IL-17, IL1R1, and PAI1), hematopoietic cell differentiation and survival (M-CSF), and fibrogenesis (PAI1, FGFb). ΔpDCs correlated with ΔIL-17 that has been reported to play a role in the development of bleomycin-induced lung fibrosis (18). Imatinib-treated patients had increased IL-1R1 that can inhibit fibroblast differentiation (19).

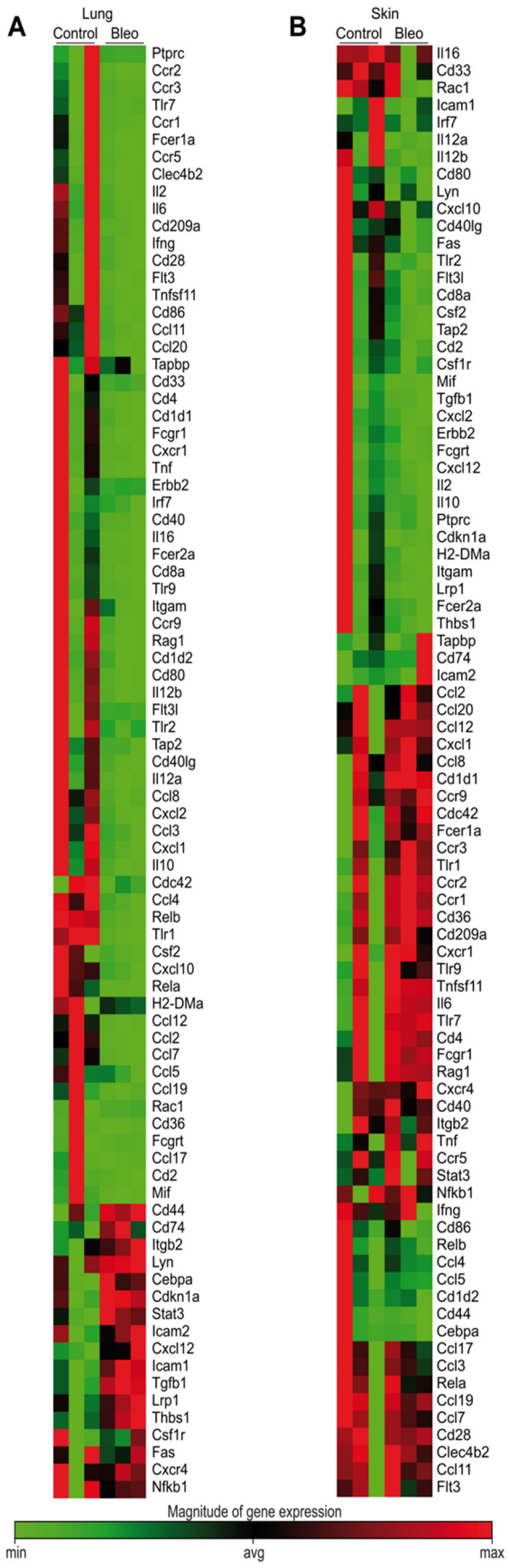

Fig. S11. Heatmap of genes expressed in the lung and skin of mice injected with bleomycin or PBS.

Animals were injected s.c. with bleomycin or PBS daily for two consecutive weeks and rested for two additional weeks. 28 d after the first bleomycin injection, lung and submandibular skin tissues from three each of PBS-injected (*Control*) and bleomycin injected (*Bleo*) mice were harvested. Total RNA was isolated, reverse transcribed, and PCR analysis conducted using the Mouse Dendritic and Antigen Presenting Cell RT^2 Profiler PCR Array (PAMM-406ZA Qiagen).

This array profiles the expression of 83 genes that have been implicated in DC activation and maturation. In addition to being functionally defined, many genes on the array are highly expressed in mature DCs or show significant changes in expression during DC differentiation.

The PCR array analysis was conducted using an iQ5 system (BioRad) according to the manufacturer's instructions. The raw array data were processed and analyzed by the PCR Array Data Analysis System, as described in Methods.

Heatmaps for all 83 genes covered in this array are shown. Results of differentially expressed genes in the lungs of PBS controls versus bleomycin-injected mice are shown in **Fig. 5**. Expression levels of none of the genes in the skin were significantly different between the bleomycin and PBS groups.

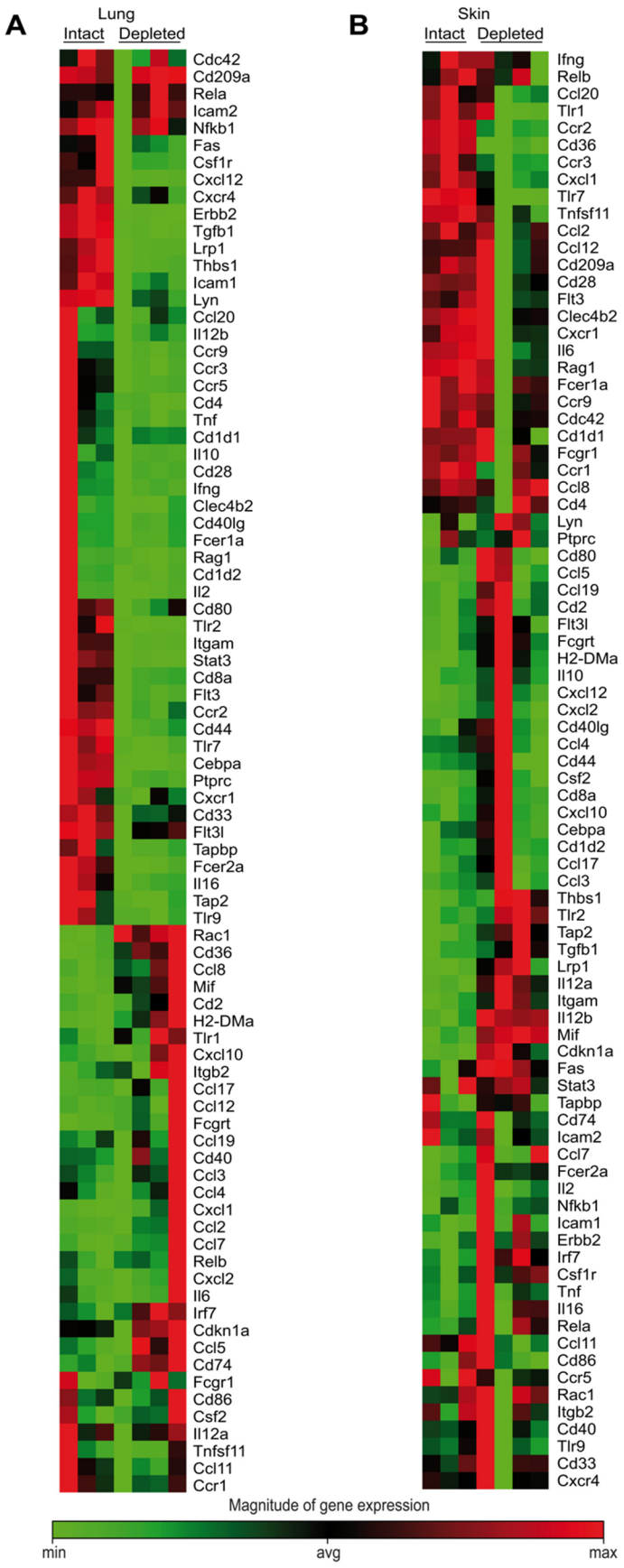

Fig. S12. Heatmap of genes expressed in the lung and skin tissue in pDC-depleted versus intact mice. Lungs and skin tissues were harvested from pDC-depleted and intact animals injected with bleomycin, as in Supplemental **Fig. S2A**. RNA was extracted from tissues, reverse transcribed to cDNA and amplified using the PCR array plates (Mouse Dendritic and Antigen Presenting Cell RT^2 Profiler PCR Array [Qiagen]), as described in **Fig. S11**.

Heatmaps are shown for all 83 genes from lung and skin tissues from 3 intact and 4 pDC-depleted mice. Results of differentially expressed genes with fold-changes and p and q values are shown in **Fig. 6.**

Supplemental Materials and Methods

Reagents for in vivo studies in animals. Bleomycin sulfate from Streptomyces verticillus was purchased from Sigma-Aldrich (St. Louis, MO). Purified anti-PDCA1 Ab (clone # JF05-IC2.41) and isotype-matched Ab (IgG2b; clone ES26-5E12.4) for *in vivo* treatment were purchased from Miltenyi Biotec (Auburn, CA).

Flow cytometry for animal studies. Single cell suspensions from mouse lung, lung-draining mediastinal or skin-draining cervical lymph nodes, skin, and spleen were obtained by mincing the tissue with scissors into pieces no larger than 2–3 mm and subsequently sieved through a 70-μm nylon filter and washed. The lung cell suspension was centrifuged at 4°C at 1500 rpm. The cell pellet was resuspended and incubated with Abs against CD16/32 for Fc receptor blockade for at least 30 min before staining. Cells were stained for 30 min at 4°C in 2% BSA PBS with 0.2mM EDTA with a combination of fluorescently-labeled Abs, washed, and analyzed on FACSCalibur or LSR-II flow cytometers (BD Biosciences). Large autofluorescent cells were excluded from the analysis. Data were analyzed with FlowJo software (TreeStar, Ashland, OR).

For flow cytometric analysis, the following fluorescent-conjugated mAbs were purchased from BD Biosciences, Tonbo Bioscience or eBioscience: B220 (RA3-6B2), CD3 (17A2 and 145-2C11), CD4 (GK1.5), CD8 (53-6.7), CD11b (m1/70), CD11c (N418), CD16/32 (93), CD19 (1D3), CD317 or PDCA-1, LAP (latency associated peptide; TW7-16B4), NK1.1 (PK136), and TCRβ (H57-597).

Antibodies and reagents for ELISA and Western blot. Pierce™ BCA protein assay kit was purchased from ThermoFisher. ELISA kits were purchased for TGFβ1 (catalog #DY1679, R&D), CXCL12 (#444207, BioLengend), and CCL2 (#88-7391-22, eBioscience). The following rabbit Ab were purchased for Western blot: TLR7 (catalog # 14-90079-81, eBioscience), Rac-1 (#SC-95, Santa Cruz Biotechnology), and C/EBPα (#2295), STAT3 (#12640), TSP-1 (#37879), LRP1 (#64099), and β-actin (#5125S) from Cell Signaling Technology.

Clinical trial of imatinib. BAL samples were obtained from patients enrolled in the "Pilot Study to Examine the Use of Imatinib (Gleevec) for the Treatment of Active Alveolitis in Systemic Sclerosis" (1) that was approved by the University of California at Los Angeles Institutional Review Board and informed consent was obtained from all the patients. At least 4 weeks before the enrollment, all putative "disease-modifying" treatments for SSc (including immunosuppressives, potassium aminobenzoate, photopheresis, colchicine, or any other experimental therapy) were discontinued. Patients were started on imatinib mesylate that was provided by Novartis Pharmaceuticals, Inc. Safety laboratory studies were performed every 2 weeks (CBC with differential counts, renal panel, hepatic panel, and urinalysis) till a stable dose was achieved and then were performed every 2 months.

Of 15 patients enrolled in the trial, one patient (#4) did not have a baseline HRCT scan and one patient (#3) did not have a post-imatinib HRCT. Seven patients completed the one-year treatment with imatinib and

eight discontinued the study. Seven of these eight patients had SSc-related or imatinib-related adverse events, and one patient was lost to follow up before completing the 12-month study.

Pulmonary function tests. Baseline measures of forced vital capacity (FVC), total lung capacity (TLC), and single-breath diffusing capacity for carbon monoxide (DLCO) were obtained on study-certified equipment in accordance with recommended standards. The quality of the tests was monitored by centralized over-reading. Serial pulmonary function tests were performed at the start of the study and every 3 months for the duration of the study.

Collection and processing of BAL and blood. 150 to 180 cc of sterile normal saline was flushed in the middle (RML) and lower (RLL) lobes of the right lung and BAL fluid was collected. Thirty ml was sent for routine laboratory analysis and the remainder was sent to our laboratory within 30 minutes of collection for cellular and protein analysis. Cells and fluid were separated and fluid was stored in 2-5 ml aliquots at -80°C. Peripheral blood was collected in green top heparin tubes. Peripheral blood mononuclear cells (PBMCs) were enriched by Ficoll gradient centrifugation and used for cellular analysis. The rest were frozen down in medium containing 90% fetal bovine serum and 10% dimethyl sulfoxide.

Flow cytometry for human samples. Cells were stained with anti-CD11c-APC, clone 3.9 (eBioscience, San Diego, CA), anti-HLA-DR-PerCP, clone G46-6 (BD Biosciences, CA), BDCA-2-FITC, clone AC144 (Miltenyi Biotec Inc.), and CD123-PE, clone 9F5 (BD Biosciences, CA) to analyze DCs. To analyze T cells, cells were stained with anti-CD3-APC, clone SK7 (BD Biosciences, CA), anti-CD4-FITC, clone RPA-T4 (BD Biosciences, CA), and anti-CD8-PEcy5, clone RPA-T8 (BD Biosciences, CA). Cells were incubated for 30 minutes at 4°C with the cell surface stains followed by permeabilization and intracellular staining with anti-IL-4-PE, clone MP4-25D2 (eBioscience, San Diego, CA), anti-IFNγ-PEcy5, clone 4S.B3 (eBioscience, San Diego, CA), and anti-IL-13-FITC, clone PVM13-1 (eBioscience, San Diego, CA) or with appropriate isotype controls, as per manufacturer's recommendations. Cells (2×10^5) were acquired on a FACSCalibur at UCLA Translational Immunology Core and data analyzed using FlowJo (Tree Star Inc., WA) software. Cell frequencies are reported as a percent of total cells.

Immunohistochemistry for human tissues. Five μm sections of paraffin-embedded tissues were stained with mouse anti-human CD303, followed by goat anti-mouse linked to horseradish peroxidase. Staining was developed with 3,3′-diaminobenzidine (DAB). Stained sections were digitized using the Aperio scanning system (Aperio Technologies; Vista, CA).

Supplemental references

1. Khanna D, Saggar R, Mayes MD, Abtin F, Clements PJ, Maranian P, Assassi S, Saggar R, Singh RR, and Furst DE. A one-year, phase I/IIa, open-label pilot trial of imatinib mesylate in the treatment of systemic sclerosis-associated active interstitial lung disease. *Arthritis Rheum.* 2011;63(11):3540-6.
2. Mostafavi S, Ray D, Warde-Farley D, Grouios C, and Morris Q. GeneMANIA: a real-time multiple association network integration algorithm for predicting gene function. *Genome Biol.* 2008;9(Suppl 1):S4.
3. Cruikshank WW, Kornfeld H, and Center DM. Interleukin-16. *J Leukoc Biol.* 2000;67(6):757-66.
4. Kaser A, Dunzendorfer S, Offner FA, Ludwiczek O, Enrich B, Koch RO, Cruikshank WW, Wiedermann CJ, and Tilg H. B lymphocyte-derived IL-16 attracts dendritic cells and Th cells. *J Immunol.* 2000;165(5):2474-80.
5. Sciaky D, Brazer W, Center DM, Cruikshank WW, and Smith TJ. Cultured human fibroblasts express constitutive IL-16 mRNA: cytokine induction of active IL-16 protein synthesis through a caspase-3-dependent mechanism. *J Immunol.* 2000;164(7):3806-14.
6. Medoff BD, Seung E, Hong S, Thomas SY, Sandall BP, Duffield JS, Kuperman DA, Erle DJ, and Luster AD. CD11b+ myeloid cells are the key mediators of Th2 cell homing into the airway in allergic inflammation. *J Immunol.* 2009;182(1):623-35.
7. Walsh ER, Sahu N, Kearley J, Benjamin E, Kang BH, Humbles A, and August A. Strain-specific requirement for eosinophils in the recruitment of T cells to the lung during the development of allergic asthma. *J Exp Med.* 2008;205(6):1285-92.
8. Fancke B, Suter M, Hochrein H, and O'Keeffe M. M-CSF: a novel plasmacytoid and conventional dendritic cell poietin. *Blood.* 2008;111(1):150-9.
9. Ebner S, Hofer S, Nguyen V, Fürhapter C, Herold M, Fritsch P, Heufler C, and Romani N. A novel role for IL-3: human monocytes cultured in the presence of IL-3 and IL-4 differentiate into dendritic cells that produce less IL-12 and shift Th cell responses toward a Th2 cytokine pattern. *J Immunol.* 2002;168(12):6199-207.
10. Ito T, Amakawa R, Inaba M, Hori T, Ota M, Nakamura K, Takebayashi M, Miyaji M, Yoshimura T, Inaba K, et al. Plasmacytoid dendritic cells regulate Th cell responses through OX40 ligand and type I IFNs. *J Immunol.* 2004;172(7):4253-9.
11. Hashizume H, Horibe T, Yagi H, Seo N, and Takigawa M. Compartmental imbalance and aberrant immune function of blood CD123+ (plasmacytoid) and CD11c+ (myeloid) dendritic cells in atopic dermatitis. *J Immunol.* 2005;174(4):2396-403.
12. Ghirelli C, Zollinger R, and Soumelis V. Systematic cytokine receptor profiling reveals GM-CSF as a novel TLR-independent activator of human plasmacytoid predendritic cells. *Blood.*115(24):5037-40.
13. Gabrielli A, Svegliati S, Moroncini G, Luchetti M, Tonnini C, and Avvedimento EV. Stimulatory autoantibodies to the PDGF receptor: a link to fibrosis in scleroderma and a pathway for novel therapeutic targets. *Autoimmun Rev.* 2007;7(2):121-6.
14. Leask A. Potential therapeutic targets for cardiac fibrosis: TGFbeta, angiotensin, endothelin, CCN2, and PDGF, partners in fibroblast activation. *Circ Res.* 2010;106(11):1675-80.
15. Loskutoff DJ, and Quigley JP. PAI-1, fibrosis, and the elusive provisional fibrin matrix. *J Clin Invest.* 2000;106(12):1441-3.
16. Liu P, Li H, Cepeda J, Zhang LQ, Cui X, Garcia JG, and Ye SQ. Critical role of PBEF expression in pulmonary cell inflammation and permeability. *Cell Biol Int.* 2009;33(1):19-30.
17. Zoppoli G, Cea M, Soncini D, Fruscione F, Rudner J, Moran E, Caffa I, Bedognetti D, Motta G, Ghio R, et al. Potent synergistic interaction between the Nampt inhibitor APO866 and the apoptosis activator TRAIL in human leukemia cells. *Exp Hematol.* 2010.
18. Wilson MS, Madala SK, Ramalingam TR, Gochuico BR, Rosas IO, Cheever AW, and Wynn TA. Bleomycin and IL-1beta-mediated pulmonary fibrosis is IL-17A dependent. *J Exp Med.* 2010;207(3):535-52.

19. Tan GH, Dutton CM, and Bahn RS. Interleukin-1 (IL-1) receptor antagonist and soluble IL-1 receptor inhibit IL-1-induced glycosaminoglycan production in cultured human orbital fibroblasts from patients with Graves' ophthalmopathy. *J Clin Endocrinol Metab.* 1996;81(2):449-52.